Title

The stomatal response to rising CO2 concentration and drought is predicted by a hydraulic trait-based optimization model.

Journal

Tree Physiology, 39(8)

ISSN

0829-318X

Authors

Wang, Yujie
Sperry, John S
Venturas, Martin D
et al.

Publication Date

2019-08-01

DOI

10.1093/treephys/tpz038

Peer reviewed

Tree Physiology 00, 1–12
doi:10.1093/treephys/tpz038

Research paper

The stomatal response to rising CO_2 concentration and drought is predicted by a hydraulic trait-based optimization model

Yujie Wang[1,3], John S. Sperry[1], Martin D. Venturas[1], Anna T. Trugman[1], David M. Love[1,2] and William R. L. Anderegg[1]

[1]School of Biological Sciences, University of Utah, Salt Lake City, 257S 1400E, UT 84112, USA; [2]Warnell School of Forestry and Natural Resources, University of Georgia, 180 E Green Street, Athens, GA 30602-2152, USA; [3]Corresponding author yujie.wang@utah.edu orcid.org/0000-0002-3729-2743

Received December 6, 2018; accepted March 22, 2019; handling Editor Annikki Mäkelä

Modeling stomatal control is critical for predicting forest responses to the changing environment and hence the global water and carbon cycles. A trait-based stomatal control model that optimizes carbon gain while avoiding hydraulic risk has been shown to perform well in response to drought. However, the model's performance against changes in atmospheric CO_2, which is rising rapidly due to human emissions, has yet to be evaluated. The present study tested the gain–risk model's ability to predict the stomatal response to CO_2 concentration with potted water birch (*Betula occidentalis* Hook.) saplings in a growth chamber. The model's performance in predicting stomatal response to changes in atmospheric relative humidity and soil moisture was also assessed. The gain–risk model predicted the photosynthetic assimilation, transpiration rate and leaf xylem pressure under different CO_2 concentrations, having a mean absolute percentage error (MAPE) of 25%. The model also predicted the responses to relative humidity and soil drought with a MAPE of 21.9% and 41.9%, respectively. Overall, the gain–risk model had an MAPE of 26.8% compared with the 37.5% MAPE obtained by a standard empirical model of stomatal conductance. Importantly, unlike empirical models, the optimization model relies on measurable physiological traits as inputs and performs well in predicting responses to novel environmental conditions without empirical corrections. Incorporating the optimization model in larger scale models has the potential for improving the simulation of water and carbon cycles.

Keywords: CO_2 concentration, drought, gain–risk optimization model, gas exchange, hydraulic risk, stomatal control.

Introduction

During the past 60 years, atmospheric CO_2 concentration has increased from 314 to 410 ppm. This accumulation of greenhouse gas has led to a 0.85 °C increase in the global mean annual temperature (IPCC 2014). The rapid temperature increase has likely exacerbated drought stress on forests in many regions, leading to episodes of drought-induced tree mortality across the globe (Adams et al. 2009, Allen et al. 2010). However, concurrent atmospheric CO_2 fertilization may mitigate the negative temperature effects on drought (Zinta et al. 2014, AbdElgawad et al. 2015, Gonzalez-Benecke et al. 2017). Fully understanding and predicting the outcomes of climate change and CO_2 fertilization on terrestrial ecosystems are contingent on models that can be used to predict responses to novel future environments (Katul et al. 2009, 2010, Medlyn et al. 2011, Chen et al. 2012, Mcdowell et al. 2013, Mackay et al. 2015, Anderegg et al. 2017, Tai et al. 2017).

A critical modeling challenge is how to represent the complexity of stomatal behavior that influences plant water loss and CO_2 uptake. To date, most land surface models rely on empirical representations of stomatal responses to environmental cues based on curve fitting to existing data sets (Ball et al. 1987, Leuning 1995, Tuzet et al. 2003, De Kauwe et al. 2013, Walker et al. 2014, Drake et al. 2017). The empirical models are computationally efficient and do not require an understanding of

[†]The present study is a revision for TP-2018-481.

the complex mechanisms underlying stomatal regulation (Chen et al. 2012, Hills et al. 2012). However, the fitted parameters of these models lack physiological or physical identities and cannot be derived explicitly from measurable plant traits (Anderegg et al. 2016, Sperry et al. 2017). Consequently, the empirical approach has a strong risk of being inadequate for accurately predicting plant responses to novel conditions (Powell et al. 2013, Anderegg et al. 2015, Drake et al. 2017, Trugman et al. 2018*b*). These models also do not directly predict the impact of drought stress on the plant's vascular transport system, the damage of which is strongly linked to the plants' drought responses and mortality risk (Sperry and Love 2015, Sperry et al. 2016, Adams et al. 2017, Trugman et al. 2018*a*).

As an alternative to the strictly empirical approach, a goal-oriented solution for stomatal behavior is potentially powerful, i.e., assuming that plants optimize water use relative to photosynthetic gain. A commonly used approach is the Water Use Efficiency Hypothesis (WUEH), which maximizes the photosynthetic gain for a given amount of water during a given time period (Cowan and Farquhar 1977). This WUEH model is a 'constrained-optimization' problem without an exact solution (Katul et al. 2009, 2010, Wolf et al. 2016, Buckley et al. 2017) and often struggles to predict accurate response to [CO_2] and soil moisture (Buckley and Schymanski 2014, Buckley 2017). The WUEH holds that stomata regulate to maintain a constant marginal water-use efficiency, λ. Katul et al. (2009, 2010) solved the optimal stomatal conductance as a function of atmospheric humidity, atmospheric [CO_2] and λ, recovering the stomatal response to atmospheric humidity used by a standard empirical approach (Medlyn et al. 2011). However, the stomatal responses to atmospheric [CO_2] and soil moisture were unrealistic unless λ is a function of both. Manzoni et al. (2013) further advanced the theory by incorporating the soil–plant limitation to leaf water supply and managed to predict realistic stomatal response to soil moisture, but did not consider the response to atmospheric [CO_2]. Thus, a perpetual challenge for the WUEH has been the need to predict λ and its dynamics in response to the full suite of fluctuating environmental stimuli, including [CO_2].

A recently proposed model assumes that the stomata regulate gas exchange so as to maximize the instantaneous carbon gain minus the risk of hydraulic failure by embolism formation (Sperry et al. 2017). The gain and risk of the stomatal opening are given equal weight, each being normalized to start from 0 at stomatal closure (no hydraulic risk but no carbon gain) and rise to 1 as stomata open (maximum photosynthesis but desiccation due to hydraulic failure). This optimization concept predicts realistic theoretic gas exchange response to environmental cues including the response to [CO_2] and soil moisture stress (Sperry et al. 2017). The gain–risk model has been shown to predict stomatal behavior and plant water status in natural droughts and research garden experiments (Anderegg et al. 2018, Venturas et al. 2018). Importantly, the gain–risk model is based on measurable plant physiological traits and hence directly calculates plant physiological status for any combination of environmental conditions, past or future.

The gain versus risk trade-off algorithm has not been fully tested under elevated [CO_2] (Venturas et al. 2018). The atmospheric [CO_2], however, is predicted to at least double to 800 ppm by the end of 21st century (RCP8.5, IPCC 2014). Thus, rigorous testing of the algorithm at elevated [CO_2] is needed to validate the model predictions of plant responses under novel future environmental conditions.

The goal of the present paper is to evaluate the gain–risk algorithm with particular emphasis on its ability to predict the response to short-term changes in [CO_2]. Experiments were conducted in a growth chamber to provide maximal control of environmental conditions. Water birch (*Betula occidentalis* Hook.) was chosen as the study species as it is relatively vulnerable to drought (Sperry and Saliendra 1994). The plants were potted to simplify the modeling of rooting depth and soil water balance. The growth chamber setting also allowed testing the modeled responses to individual stimuli in isolation ([CO_2], relative humidity (RH) and soil drought), which was not possible to do in the research garden experiment (Venturas et al. 2018). The ability of the gain–risk model to predict the experimental results was compared with a standard empirical stomatal model (Medlyn et al. 2011) parameterized to the best fit the same experimental data.

Materials and methods

Plant materials

Water birch (*B. occidentalis* Hook.) trees were grown from seedlings in the greenhouse of the School of Biological Sciences, University of Utah (40° 45′ 48.75″ N, 11° 50′ 57.66″ W, 1425 m above sea level) starting in October 2016. Each tree was grown in a 5-gallon pot with local sandy clay loam soil. Plants were well watered and day length was regulated to 10 h from 8:00 a.m. to 6:00 p.m. with supplemental light (Lucalox LU1000, GE Lighting, East Cleveland, Ohio, USA). In February 2017, 2 weeks prior to the experiments, 10 trees (1–1.5 m tall, 2 years old) were moved into a growth chamber (Model PR-915, Percival Scientific, Perry, Iowa, USA) in order to acclimate the trees to the growth chamber environment. The growth chamber was set at the default settings of ambient CO_2 concentration at 400 ppm, air temperature at 25 °C, RH at 55%, light intensity (photosynthetic active radiation, PAR) at 1000 μmol m^{-2} s^{-1} and day length at 10 h (from 8:00 a.m. to 6:00 p.m. local time). Trees were watered with 1 l water at the end of each day until the drought experiment was initiated.

Experimental design

Growth chamber trees were subjected to three sequential treatments: ambient CO_2 concentration, RH and soil drought. The responses of leaf xylem pressure and leaf gas exchange were measured during each treatment. The CO_2 treatment was conducted on six trees (trees no. 1–6) at a series of ambient CO_2 concentrations starting at 800 ppm, and stepping down to 600, 400, 300 and 200 ppm. All other environmental conditions were kept at default settings. Trees were held at each concentration for at least 90 min prior to measurements. The CO_2 response was measured from high to low [CO_2] in order to avoid any legacy impact of cavitation due to more negative leaf xylem pressures at lower [CO_2]. At the end of the experiment, the chamber [CO_2] was returned to the default at 400 ppm.

Next, the RH treatment was conducted on six trees (trees no. 1, 2 and 7–10) at a series of RH settings of 75%, 65%, 55%, 45% and 35% while keeping other environmental conditions at default settings. The actual chamber vapor pressure deficit (air VPD) was estimated for each gas exchange measurement based on spot measurements of RH and air temperature. The humidity response was measured going from high to low RH in order to avoid the potential legacy of cavitation due to lower leaf xylem pressure in drier air. A different set of trees were chosen for the RH (and soil drought, below) treatments to decrease the reduction in leaf area caused by sampling for pressure chamber measurements of xylem pressure. After the RH experiment, the chamber RH was set back to the default 55%.

The final drought response experiment was also performed on six trees (trees no. 2, 4, 6 and 8–10). Trees were watered only on the first day and dried for four successive days, with measurements conducted at the end of the day. After the measurements, trees were bagged and placed in the dark for at least 3 h to suppress transpiration and equilibrate leaf xylem pressure with soil water potential. Leaf xylem pressure was measured on two to three leaves for each bagged tree and served as a proxy for the soil water potential at the end of the day. Trees were then moved back into the growth chamber for further drought. The growth chamber conditions and timing for leaf xylem pressure measurements of the CO_2, RH and drought treatments are listed in supplementary data Table S1 (available as Supplementary Data at *Tree Physiology* Online).

The tree response to each treatment (CO_2, RH, soil drought) was assessed from measurements of gas exchange and xylem pressure. Gas exchange measurements were performed only when the light had been turned on for at least 120 min and when the growth chamber environment had stabilized for 90 minutes. The whole-tree transpiration rate (E_{tree}) was measured with a 0.5 g precision 34 kg range balance (Sartorius LP34000P, Sartorius Corporation, Goettingen, Germany). The total weight was recorded to the computer every 10 s for 6–10 min. Whole-tree transpiration rate was estimated from the slope of the linear regression of weight loss versus time. Leaf level gas exchange (including photosynthetic rate, stomatal conductance and leaf temperature, T_{leaf}) was measured on two to four leaves on each tree at each treatment stage with a portable photosynthesis system (Li-6800, LICOR Inc., Lincoln NE, USA) by setting the Li-6800 chamber temperature at the growth chamber temperature. One of the leaves used in the photosynthesis measurement was then used in the leaf xylem pressure measurement with a pressure chamber (PMS Instruments, Corvallis, OR, USA; precision ±0.05 MPa) for each tree at different stages of three treatments. Transpiring leaf xylem pressures were measured only for three stages in each treatment in order to minimize the disturbance of decreased leaf area.

Model description

The gain–risk model (Sperry et al. 2017) was modified for the input/output of this study (Table 1). The model was coded with Julia (Julia 0.4.7, NumFocus) and is publicly available (https://github.com/Yujie-WANG/Published-Codes-Yujie-WANG). The plant was represented by one canopy sunlit layer, one stem element, one root layer and one rhizosphere and soil layer in series. No shaded canopy layer was modeled because there was no significant leaf shading for the small saplings (1.0–1.5 m tall) in the growth chamber, and only one root layer was used due to the homogeneous soil moisture in a small pot. Leaf temperature was not modeled in this version because the main purpose of the study was to test the accuracy of the optimization algorithm itself rather than the additional energy balance routine that predicts T_{leaf} in the full version (Sperry et al. 2017, Venturas et al. 2018). Instead, the T_{leaf} required by the model was an input and was averaged from the T_{leaf} measurements for each tree. The model simulations assumed that cavitation of xylem conduits was irreversible (no xylem refilling). Examples of how xylem water pressure and hydraulic conductivity loss respond to the environmental cues can be found in Figure S1 (available as Supplementary Data at *Tree Physiology* Online).

The gain–risk model calculates the relative photosynthetic gain and hydraulic risk of stomatal opening at each time step. The gain is the photosynthetic rate relative to the maximum possible achieved by stomata opening at that time step. Maximal carboxylation rate at 25 °C (V_{cmax}), maximal electron transport at 25 °C (J_{max}), air temperature, T_{leaf}, PAR and ambient [CO_2] are the necessary inputs for computing the photosynthetic gain (Table 1). The risk function measures the relative loss of hydraulic conductance at the end of the transpiration stream, which rises from 0 at stomatal closure to 1 for complete failure at the runaway cavitation. Necessary inputs include the soil moisture, rhizosphere resistance, vulnerability curves (VCs) and maximal conductances of the root, stem and leaf elements of the flow path, as well as the leaf area per basal area (Table 1). Once the gain and risk functions are calculated as a function

Table 1. List of symbols, definitions and status as model input or output. Note that leaf temperature and soil water potential are used as input in this model to test the gain–risk algorithm while they are used as outputs in other versions of the model (Venturas et al. 2018).

Symbol	Definition	Unit	Input/output
A	Photosynthetic assimilation, photosynthetic rate	μmol CO_2 m^{-2} s^{-1}	Output
C_a	Atmospheric CO_2 concentration	ppm	Input
C_i	Intercellular CO_2 concentration	ppm	Output
D	Leaf-to-air vapor pressure deficit	kPa	–
E_{tree}	Transpiration rate of the tree per basal area	kg h^{-1} m^{-2}	Output
J_{max}	Maximal electron transport at 25 °C	μmol CO_2 m^{-2} s^{-1}	Input
K_{max}	Maximal tree hydraulic conductance	kg h^{-1} MPa^{-1} m^{-2}	Input
K_{rhizo}	Maximal tree rhizosphere conductance	kg h^{-1} MPa^{-1} m^{-2}	Input
La:Ba	Leaf area to basal area ratio	m^2 m^{-2}	Input
MAPE	Mean absolute percent error	%	–
PAR	Photosynthetic active radiation	μmol m^{-2} s^{-1}	Input
P_{leaf}	Leaf xylem pressure under light condition	MPa	Output
P_{pd}	Predawn leaf xylem pressure, a proxy for soil water potential	MPa	–
P_{soil}	Soil water potential	MPa	Input
RH	Relative humidity	%	–
T_{leaf}	Leaf temperature	°C	Input
VC	Xylem vulnerability curve to cavitation	–	Input
V_{cmax}	Maximal carboxylation rate at 25 °C	μmol CO_2 m^{-2} s^{-1}	Input
VPD	Vapor pressure deficit in the air	kPa	Input
Weibull B	Fitting parameter of the VC Weibull function	−MPa	Input
Weibull C	Fitting parameter of the VC Weibull function	–	Input

of stomatal opening, the optimization algorithm finds the point at which the gain minus risk difference is maximized. This predicts the gas exchange and water status parameters (e.g., photosynthetic rate, transpiration rate, leaf xylem pressure) at the time step. Model details can be found in Sperry et al. (2017) and Venturas et al. (2018).

Measuring model input parameters

Photosynthesis parameters V_{cmax} and J_{max} at 25 °C were obtained from the measured relationship between the photosynthetic rate (A) and intercellular CO_2 concentration (C_i), A–C_i curves. These curves were obtained for each tree in the growth chamber prior to each experimental treatment. For each curve, the net photosynthetic rates were measured at the leaf temperature of 25 °C and light intensity of 1000 μmol m^{-2} s^{-1} under a series of CO_2 concentrations: 50, 100, 150, 200, 300, 400, 500, 600, 800, 1000, 1200, 1400, 1600, 1800 and 2000 ppm. The dark respiration rate was then measured at the leaf temperature of 25 °C and PAR = 0. The gas exchange measurements were done with a portable photosynthesis system (Li-6800). A–C_i curves were fitted to obtain the V_{cmax} and J_{max} with the *scipy.optimize.leastsq* module in Python 3.6.5 (code provided with the gain–risk model). A total of 43 A–C_i curves were constructed for the 10 trees and the average V_{cmax} and J_{max} for each tree were calculated and used as model input. Ambient [CO_2] and light were recorded from the growth chamber. Leaf temperatures were recorded from the Li-6800 where the inlet air temperature was set to the chamber air temperature.

Vulnerability curves for the root and stem Vulnerability curves of root, stem and leaf were constructed from well-watered, greenhouse-grown trees of the same cohort for the growth chamber experiments. Branches ∼80 cm long and roots were harvested, wrapped with black plastic bags and transported to the lab within 5 min of the collection. Stem and root segments 16–20 cm long were cut under water. The segments were vacuum infiltrated in 10 mM KCl for 30 min to remove the emboli in vessels. The segments were trimmed to 13.8 cm and maximal hydraulic conductivity was measured with a conductivity apparatus (Sperry et al. 1988). Stem and root segments were then spun in a custom built rotor in a centrifuge for 10 min to introduce embolism under different pressures (Alder et al. 1997). Hydraulic conductivity was measured immediately after taking the segment out of the centrifuge by correcting the background flow (Hacke et al. 2000, Torres-Ruiz et al. 2012). Each segment was only used to measure the maximal conductivity and conductivity after spinning in the centrifuge (single spin method, Hacke et al. 2015). A total of 39 stem segments and 24 root segments were used to construct the VCs for stem and root, respectively. Root and stem VCs were fitted to the Weibull function, $k = k_{max} \times \exp[-(P/B)\hat{}C]$, where k_{max} is the maximal hydraulic conductance of the element, B and C are the fitted Weibull parameters and P is the xylem pressure in MPa.

Vulnerability curve for the leaf Potted trees in the greenhouse were dried to different leaf xylem pressures and then transported to the lab. Leaf xylem pressure was measured

on two to three bagged leaves for each stressed tree and then a leafy branch (basal diameter >5 mm) was harvested from the tree. Leaf edges were trimmed to expose the minor veins. The hydraulic conductance of the branch (k_{br}) was measured using the vacuum chamber method (Kolb et al. 1996). Then leaves were cut from the branches at the proximal base of the petiole and hydraulic conductance of the stem (k_{st}) was measured under a series of vacuum pressures. The hydraulic conductance of the leaf xylem was computed as $k_{lf} = 1/(1/k_{br} - 1/k_{st})$. The leaf VC was constructed with 31 branches by plotting the k_{lf} versus leaf xylem pressure and fitting the Weibull function.

Maximal tree hydraulic conductance and its partitioning

The whole-tree K_{max} per basal area represents the hydraulic conductance in the absence of any embolism. It was back-calculated from measured tree conductance under well-watered conditions, based on the VCs (Sperry and Love 2015, Venturas et al. 2018). Tree conductance (per growth chamber tree) was the quotient of measured midday transpiration rate and the difference between midday leaf xylem pressure and predawn leaf xylem pressure. The Python script to solve for K_{max} from measured tree conductance can be found along with the model code.

The K_{max} had to be partitioned into root, stem and leaf components (the rhizosphere resistance under wet soil conditions is negligible). The fraction of tree hydraulic resistance (reverse of conductance) in the roots was computed as $(P_{md,b} - P_{pd})/(P_{md} - P_{pd})$, where P_{pd} is the predawn leaf xylem pressure, $P_{md,b}$ is midday bagged leaf xylem pressures of leaves inserted near the root crown and P_{md} is midday xylem pressure of transpiring leaves in the canopy. The stem versus leaf resistance ratio was obtained from the vacuum method, i.e., k_{lf}/k_{st}. The resistance ratios of the stem and leaf to the whole tree were calculated as $(P_{md} - P_{md,b})/(P_{md} - P_{pd}) \times k_{lf}/(k_{lf} + k_{st})$ and $(P_{md} - P_{md,b})/(P_{md} - P_{pd}) \times k_{st}/(k_{lf} + k_{st})$, respectively.

Leaf area and stem area

After the experimental treatments were concluded in the growth chamber, the 10 experimental trees were cut to measure the leaf area and stem area. All the shoots were cut from the trees; leaf area and stem area were measured to obtain the leaf area to stem area ratio (La:Ba). Leaf areas were measured with a leaf area meter (Li-3100, LICOR Inc. Lincoln NE, USA). Three out of 10 trees (trees no. 3, 5 and 7) had a smaller La:Ba while 7 out of 10 trees (trees no. 1, 2, 4, 6 and 8–10) had a bigger La:Ba, so two different average ratios were computed for these two subsets and used as model input. Stem basal area was summed from the shoots in the pot. The average leaf area per basal area and stem basal area per tree were used to convert between leaf area-specific versus whole-tree transpiration rate.

Rhizosphere resistance

The hydraulic conductance in the rhizosphere (K_{rhizo}) cannot be measured directly. The rhizosphere conductance was obtained from the value that minimized the sum of standardized square error (i.e., the sum of [measured − modeled/mean measured]^2) of leaf xylem pressure, transpiration rate and photosynthetic rate across all comparisons in the CO_2, RH and drought treatments (90 observations in total).

Soil moisture

For the CO_2 and RH treatments, 'predawn' leaf xylem pressure (a proxy for soil water potential) was measured with a pressure chamber in the early morning before the lights were turned on. Trees were bagged during the night to ensure the suppression of nocturnal transpiration. The P_{pd} was measured for each tree in the CO_2 and RH treatments and was assumed to be constant throughout the treatment day. For the drought treatment, the soil water potential was assessed from 'predawn' xylem pressures measured at the end of each drought day as already described.

Testing the gain–risk model

The gain–risk model was run for each tree for the same set of environmental conditions corresponding to the measurement of the tree's response to CO_2, RH or drought. The predicted transpiration rate (E_{tree}), photosynthetic rate (A) and leaf xylem pressure (P_{leaf}) were compared with experimental observations to evaluate the model performance in predicting the stomatal responses to environmental cues. The comparison was quantified by calculating the mean absolute error (MAE) and mean absolute percentage error (MAPE; mean absolute difference as a percentage of the observed mean) for each comparison of A, E_{tree} and P_{leaf} for each treatment. Errors were equally weighted across the three variables by studentizing each value (subtracting the observed mean and dividing by the observed standard deviation). Model performance per treatment (CO_2, RH, soil drought) was averaged from the MAPE for the A, E_{tree} and P_{leaf} response obtained for each treatment. Model performance per variable was the variable's MAPE averaged over all treatments. The overall model performance was evaluated by the MAPE averaged across all three variables and treatments.

Comparison with an empirical model

For comparison with the widely used empirical approach for modeling plant water status and gas exchange, a standard version of Ball–Berry–Leuning–Medlyn-type model was used (Ball et al. 1987, Leuning 1995, Medlyn et al. 2011). For the empirical model, stomatal conductance, g_s, was predicted as

$$g_s = g_0 + \frac{1.6A}{C_a} \bullet \left(1 + \frac{g_1}{\sqrt{D}}\right) \bullet \left(\frac{P_{soil} - P_{min}}{P_{max} - P_{min}}\right), \quad (1)$$

where C_a is atmospheric [CO_2], D is the leaf-to-air vapor pressure deficit, g_0, g_1, P_{min} and P_{max} are four parameters

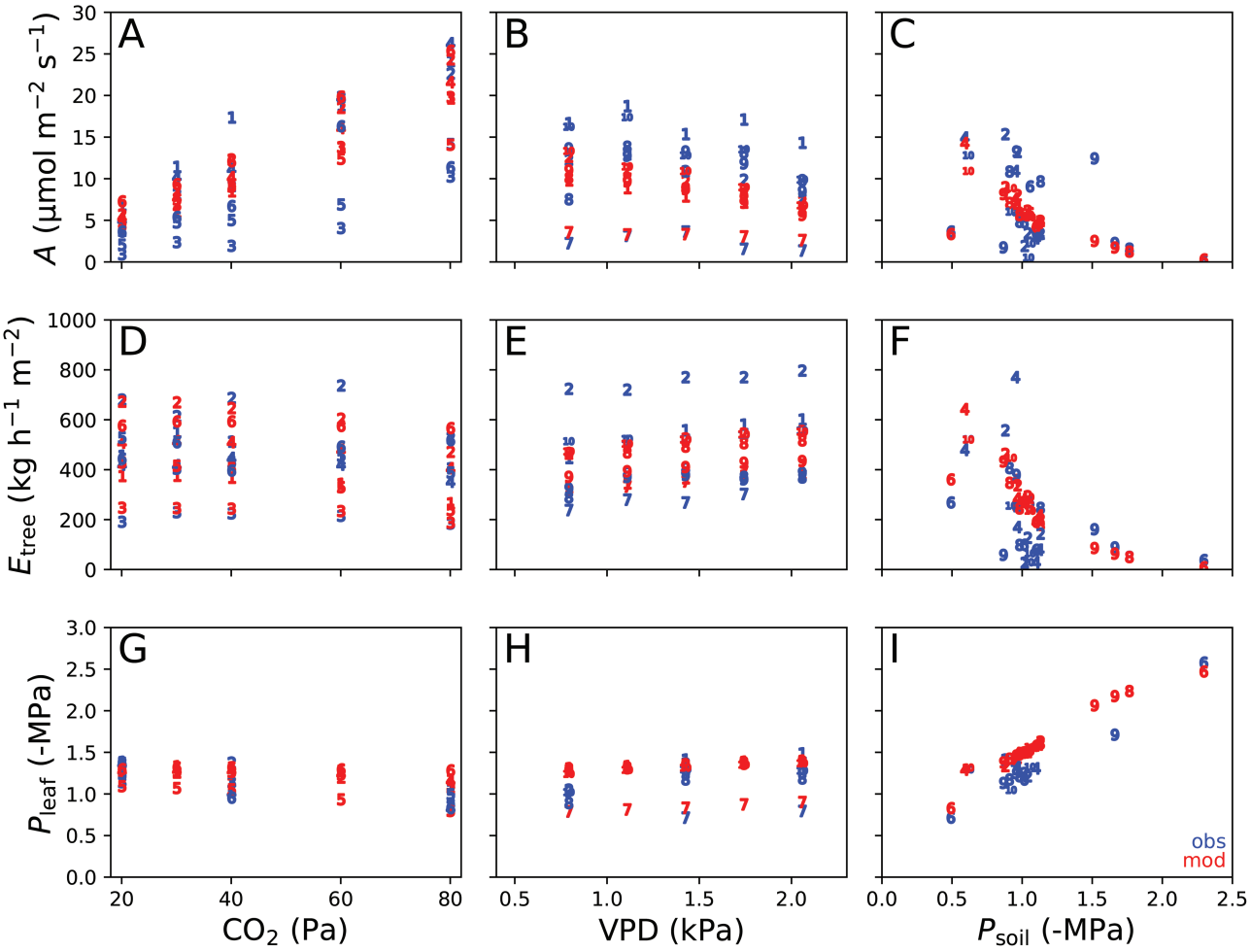

Figure 1. Observations and gain–risk model predictions in the CO_2, humidity and drought treatments. The blue numbers show the observations while the red numbers show the model prediction of each tree (identification number from 1 to 10). Panels (A)–(C) show the observed and modeled photosynthetic rate (A). Panels (D)–(F) show the observed and modeled tree transpiration (E_{tree}). Panels (G)–(I) show the observed and modeled leaf xylem pressure (P_{leaf}). The VPD is the vapor pressure deficit in the air.

fitted to the data and P_{soil} is the soil water potential (predawn leaf xylem pressure was the proxy for P_{soil}). Standard empirical stomatal conductance models lack a soil moisture term (e.g., the right-hand bracketed term; Ball et al. 1987, Leuning 1995, Medlyn et al. 2011), which is added to account for drought stress in large-scale ecosystem models (Trugman et al. 2018b). Equation 1 without the soil moisture term is consistent with the WUEH (Cowan and Farquhar 1977) assuming that RuBP regeneration governs the photosynthesis and marginal water use efficiency is independent of C_a and P_{soil}. The solution of Eq. 1 must also satisfy the physiological relationship between g_s and A, which was assumed to be identical to the gain function for consistency with the gain–risk model (g_s and A were calculated from the intersection of the A–C_i curve and Eq. 1). Similarly, g_s was linked to E_{tree} and P_{leaf} as dictated by the risk function. The fitting parameters were optimized to minimize the sum of studentized MAE (measured versus modeled A, E_{tree} and P_{leaf}; values were studentized by subtracting the observed mean and dividing by the observed standard deviation) for combined [CO_2], RH and drought treatments. Once parameterized, Eq. 1 was numerically solved for the g_s and associated A, E_{tree} and P_{leaf} that satisfied the gain and risk function specific to each tree and measurement period. The code for the empirical model is available at https://github.com/Yujie-WANG/Published-Codes-Yujie-WANG.

Results

Plant traits and model inputs

Mean V_{cmax} for each tree ranged from 12.8 to 96.6 μmol m^{-2} s^{-1} and mean J_{max} ranged from 24.0 to 203.0 μmol m^{-2} s^{-1}. J_{max} was linearly correlated with V_{cmax} (R^2 = 0.992, N = 43) with a ratio of 1.86 (see Figure S2 available as Supplementary Data at *Tree Physiology* Online). Trees no. 3, 5 and 7 had significantly lower leaf area to basal area ratio averaging 2648 m^2 m^{-2} compared with the rest of the trees, which averaged 5663

m^2 m^{-2}, and the model was parameterized accordingly. The average percentage of tree hydraulic resistance in root, stem and leaf pathways was 53.7%, 24.3% and 22.0%, respectively. Estimated rhizosphere conductance was 6×10^8 times the K_{max} of each tree (yielding an average rhizosphere resistance of 36.2% over the full range of soil water potential from zero to the value at which gas exchange would cease). The K_{max} of each tree ranged from 560 to 1970 kg h^{-1} MPa^{-1} m^{-2}. Roots and leaves were more vulnerable to cavitation than the stems with the P_{50} (xylem pressure at 50% loss of conductance) of −1.14 MPa and −1.10 MPa, respectively, compared with the −1.97 MPa in stems. The traits used for modeling each tree can be found in the supplementary data (see Table S2 available as Supplementary Data at *Tree Physiology* Online).

Performance of the gain–risk model

In the CO_2 experiment, as CO_2 concentration was decreased from high (800 ppm) to low (200 ppm), the observed photosynthetic rate decreased ($P < 0.001$, linear regression, Figure 1A, blue data), whole tree transpiration increased non-significantly ($P = 0.13$, linear regression, Figure 1D, blue data) and leaf xylem pressure became more negative ($P = 0.03$, linear regression, Figure 1G, blue data). The gain–risk model tracked these measured trends well (Figure 1A,D, and G, red data). The standardized MAPE was 25.0%, averaged across all photosynthesis, transpiration and leaf xylem pressure comparisons (Figure 2A, Table 2). The error was lower for the predictions of transpiration and xylem pressure than for photosynthesis (Table 2). The linear regression slope for modeled versus measured transpiration was not significantly different from 1 ($P = 0.14$, Table 2), and the rest of the variable sets had slopes significantly shallower than 1 ($P < 0.001$, Table 2).

In the RH treatment, as RH was decreased from high to low (from 75% to 35%, corresponding to an atmospheric VPD ranging from 0.79–2.06 kPa), the observed photosynthetic rate decreased ($P < 0.001$, linear regression, Figure 1B, blue data) while tree transpiration rate increased ($P = 0.05$, linear regression, Figure 1E, blue data) and leaf xylem pressure became more negative ($P = 0.84$, Figure 1H, blue data). The gain–risk model tracked these trends (Figure 1B, E and H red data) with an overall MAPE of 21.9% (Figure 2B). The error was greatest for photosynthesis and least for xylem pressure (Table 2). The linear regression slope for each modeled versus measured variable set (i.e., A, E_{tree}, P_{leaf} and All) was significantly lower than 1 ($P < 0.001$, Table 2).

In the soil drought treatment, as predawn xylem pressure fell from −0.5 MPa to −2.3 MPa during the drought, the observed photosynthesis, transpiration and leaf xylem pressure fell ($P < 0.001$, linear regression, Figure 1C, F and I, blue data). These trends were predicted by the gain–risk model (Figure 1C, F and I, red data), but the percentage error was greater at 41.9% (Figure 2C). The percentage error was larger for photosynthesis and transpiration than xylem pressure (Table 2). The larger percentage error in the drought treatment compared with the CO_2 and RH treatments resulted from the lower mean photosynthesis and transpiration rates measured under drought stress. In terms of average absolute value of the error, the drought treatment was comparable to the [CO_2] and RH treatments. The linear regression slopes for the modeled versus measured transpiration and leaf xylem pressure were not significantly different from 1 ($P = 0.58$ and 0.13, respectively, Table 2), but the slopes for photosynthesis and combined variable set were significantly lower than 1 ($P < 0.001$, Table 2).

Pooling the CO_2, RH and soil drought treatments, the overall MAPE for the gain–risk model was 26.8% (Figure 2D), with more error in the photosynthesis prediction (38.1%) than the xylem pressure prediction (14.5%). Transpiration MAPE was intermediate (27.8%, Table 2). The model predictions fell close to the 1:1 line that was also within the 95% confidence limits of the regression. A linear regression of the studentized model prediction versus observations had slope lower than 1 for each treatment, each variable and combined treatments ($P < 0.01$, Figure 2A–D, Table 2).

Comparison with the empirical model

Pooling across all treatments and variables, the gain–risk model predicted observed tree responses more skillfully (MAPE = 26.8%) than the Ball–Berry–Leuning–Medlyn empirical model (MAPE = 37.5%; Figure 2D and H). On a per treatment basis, the gain–risk model gave lower errors for all the [CO_2], RH and drought responses (Figure 2A–C, E–G). Per variable, the gain–risk model better predicted the photosynthesis, whole-tree transpiration and leaf xylem pressure for combined treatments. The empirical model only performed slightly better for photosynthesis in the [CO_2] treatment and whole-tree transpiration in the drought treatment (Table 2). A linear regression of the studentized empirical fitting had slope lower than 1 for each treatment and combined treatments ($P < 0.001$, Figure 2E–H, Table 2). Per variable, only the linear regression for leaf xylem pressure in the RH, drought and all treatments combined showed slopes not significantly different from 1 ($P = 0.34$, 0.91 and 0.76, respectively, Table 2). In the RH treatment, the empirical model underestimated A, E_{tree} and P_{leaf} as the modeled values were below the 1:1 line (Figure 2F).

Discussion

The gain–risk optimization model was able to capture the [CO_2], air humidity and soil drought responses in novel conditions, suggesting that patterns of tree-level gas exchange are consistent with an optimization of carbon gain and hydraulic risk. The gain–risk model showed better overall predicting power than

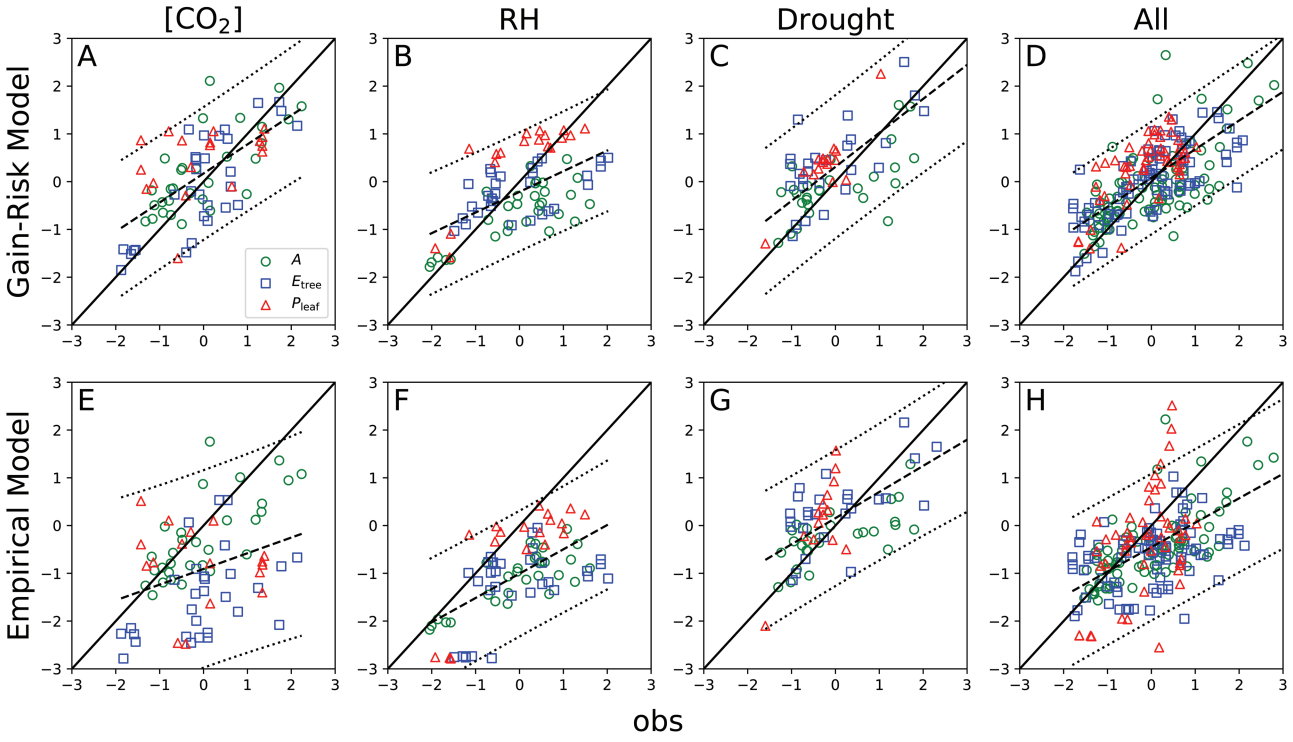

Figure 2. Comparison of model predictions of studentized photosynthesis (A, green circle), transpiration (E_{tree}, blue square) and leaf xylem pressure (P_{leaf}, red triangle) versus experimental observations. Panels (A)–(D) show the gain–risk model predictions for CO_2, RH, drought and all treatments, respectively. Panels (E)–(H) show the empirical model fittings for CO_2, RH, drought and all treatments, respectively. Solid black lines are the 1:1 relationship. Dashed lines are the regression lines. Dotted lines are the 95% confidence intervals for the linear regression. The mean absolute percentage error and the regression statistics are listed in Table 2.

the empirical model, which had the advantage of freely tuning four parameters to best fit the data. The only parameter adjusted post-hoc in the gain–risk approach was the rhizosphere conductance, which is a difficult trait to measure. This trait selectively influences the model under drought conditions because only in drying soil does rhizosphere hydraulic conductance become limiting (Sperry et al. 1998, Sperry and Love 2015, Wolfe et al. 2016). Thus, the post-hoc adjustment of the rhizosphere conductance had a minimal influence on the good fits observed in the well-watered CO_2 and RH treatments. The advantage of having all model parameters associated with identifiable traits is that this makes it easier to assign a value and uncertainty to them a priori when true predictions are required (as opposed to the hind-casting that is possible during model validation). One can also better understand the physiological basis for uncertainties in model projections when all inputs are linked to trait and process. At the same time, it is important to restrict the model to well-understood trait and process, or risk regression to post-hoc fitting that becomes equivalent to the empirical approach. For example, it can be conceptually useful to incorporate phloem transport in an optimization model, but this approach has the downside of adding a suite of currently poorly known parameters (Nikinmaa et al. 2013, Huang et al. 2018).

The present results add to the prior validations of the gain–risk algorithm in controlled plantation experiment with aspen (*Populus tremuloides*; Venturas et al. 2018), and meta-analysis of gas exchange data from a variety of species (Anderegg et al. 2018). The work adds to this body of literature and is the first testing of the model's CO_2 response to both elevated and decreased CO_2 concentrations. The overall error (26.8% for all treatments) was comparable to that for the Venturas et al. (2018) study (27.9% for control and drought treatments). Although the percentage error was higher for the drought treatment (41.9%), this was owing to lower mean values rather than to a greater absolute error. The MAEs for water birch (A: 2.83, E_{tree}: 135.52 and P_{leaf}: 0.23 for drought treatment, units in Table 1) were comparable to the MAEs for aspen in the Venturas study (A: 2.3, E_{tree}: 151.2 and P_{leaf}: 0.4, units in Table 1). An advantage of the growth chamber experiments was the ability to isolate the model error for each individual driver ($[CO_2]$, RH and soil drought). Similar absolute error values indicated that the gain–risk model represented all responses with equal fidelity (Table 2).

The slope of the model predictions and observations in Figure 2D was significantly lower than 1, suggesting that the model either underestimated gas exchange rates under

Table 2. The comparison of gain–risk model and empirical model predictions. MAE (units for A, E_{tree} and P_{leaf} reported in Table 1) and MAPE stand for mean absolute error and mean absolute percentage error, respectively. The row 'slope' denotes the slope of the regression between observed values (x) and modeled values (y). The row 'slope = 1' denotes the P-value for the linear regression slope being different from 1. Units as in Table 1.

Treatment/Model		Predicted			
		A	E_{tree}	P_{leaf}	All
CO_2/Gain–risk	MAPE	41.1%	17.8%	16.2%	25.0%
	MAE	4.25	78.83	0.18	
	Slope	0.62 ± 0.11	0.81 ± 0.12	0.25 ± 0.15	0.61 ± 0.08
	Slope = 1	0.00	0.14	0.00	0.00
	R^2	0.527	0.606	0.140	0.441
CO_2/Empirical	MAPE	40.7%	49.1%	26.7%	38.8%
	MAE	4.21	217.29	0.30	
	Slope	0.63 ± 0.11	0.36 ± 0.16	−0.23 ± 0.24	0.33 ± 0.12
	Slope = 1	0.00	0.00	0.00	0.00
	R^2	0.539	0.155	0.059	0.094
RH/Gain–risk	MAPE	31.5%	23.5%	10.7%	21.9%
	MAE	3.50	111.66	0.12	
	Slope	0.45 ± 0.08	0.25 ± 0.07	0.71 ± 0.11	0.43 ± 0.07
	Slope = 1	0.00	0.00	0.02	0.00
	R^2	0.563	0.287	0.708	0.332
RH/Empirical	MAPE	46.9%	41.7%	14.0%	34.2%
	MAE	5.20	198.18	0.16	
	Slope	0.45 ± 0.07	0.37 ± 0.12	0.85 ± 0.16	0.51 ± 0.07
	Slope = 1	0.00	0.00	0.34	0.00
	R^2	0.632	0.237	0.651	0.382
Drought/Gain–risk	MAPE	43.0%	65.4%	17.3%	41.9%
	MAE	2.83	135.52	0.23	
	Slope	0.44 ± 0.10	0.91 ± 0.17	0.85 ± 0.10	0.71 ± 0.09
	Slope = 1	0.00	0.58	0.13	0.00
	R^2	0.421	0.544	0.849	0.483
Drought/Empirical	MAPE	45.5%	59.2%	21.7%	42.1%
	MAE	2.99	122.56	0.29	
	Slope	0.36 ± 0.08	0.45 ± 0.12	1.02 ± 0.20	0.55 ± 0.09
	Slope = 1	0.00	0.00	0.91	0.00
	R^2	0.446	0.373	0.658	0.381
All/Gain–risk	MAPE	38.1%	27.8%	14.5%	26.8%
	MAE	3.58	106.58	0.17	
	Slope	0.56 ± 0.07	0.54 ± 0.05	0.79 ± 0.07	0.60 ± 0.04
	Slope = 1	0.00	0.00	0.01	0.00
	R^2	0.463	0.541	0.690	0.506
All/Empirical	MAPE	44.2%	47.6%	20.7%	37.5%
	MAE	4.17	181.80	0.25	
	Slope	0.51 ± 0.06	0.25 ± 0.07	0.95 ± 0.15	0.51 ± 0.05
	Slope = 1	0.00	0.00	0.76	0.00
	R^2	0.479	0.153	0.455	0.304

favorable conditions or overestimated them under stressful conditions. The results suggest that the latter case applies to the water birch because the model predicted leaf xylem pressure became overly negative under stressed conditions (Figures 1F and I, and 2C). This behavior would occur if the measured leaf VC was more resistant than the actual leaf VC. An overly resistant leaf VC would lead to more negative predicted P_{leaf} and higher predicted transpiration at any soil moisture condition (Figures 1F and I, and 2C). The measured leaf VC was for leaf xylem only, and so excluded potential declines in leaf hydraulic conductance in the extra-xylary flow path. The response of extra-xylary hydraulic conductance to water stress requires more quantitative investigation (Bartlett et al. 2014, Meinzer et al. 2016, Scoffoni et al. 2017) and may improve model performance. Incorporating the mesophyll conductance in the model may also improve the predictions (Dewar et al. 2018, Flexas et al. 2008), but there are still knowledge gaps that prevent incorporating it in the gain–risk model such as how

to quantifiy the change of mesophyll conductance in response to the environment.

The empirical approach performed less satisfactorily compared with the trait-based gain–risk model, especially in predicting E_{tree} and P_{leaf} in the CO_2 and RH treatments (Table 2). The underperformance of the empirical model was despite the advantage of fitting model parameters to the observed data set and using the same linkage between g_s, A, E_{tree} and P_{leaf} employed in the gain–risk model (i.e., the gain and risk functions). Either the model 'parameters' are not constants as intended or the empirical equation itself does not fully capture the complexity of the stomatal response to CO_2, RH and soil drought. Even if an empirical approach had been as successful as the gain–risk model, as was the case in the aspen study of Venturas et al. (2018), the gain–risk model has the advantage of being parameterized by measurable traits with known uncertainties. The gain–risk approach also capitalizes on the known linkage between stomatal behavior and physiological traits (Pataki et al. 1998, Sperry 2000, Hubbard et al. 2001, Santiago et al. 2004).

While the gain–risk model can predict well the stomatal behavior based on measured traits, the predictions may only be relevant for short timeframes when these measured traits stay unchanged. Acclimation such as changes in leaf respiration, leaf area per basal area, photosynthetic capability and rooting depth has the potential to change plant response over time to the long-term changes in [CO_2], temperature and other factors (Eissenstat et al. 2000, Ainsworth and Long 2005, Guswa 2008). The fact that the gain–risk model is trait-based allows for modeling these acclimation processes as they become better understood. In conclusion, the gain–risk model appears to hold promise for improving predictions of forest health in response to a changing climate.

Conflict of interest

None declared.

Funding

This study was funded by NSF 1450650 granted to J.S.S. W.R.L.A. acknowledges funding from the David and Lucille Packard Foundation, the University of Utah Global Change and Sustainability Center, NSF Grants 1714972 and 1802880, and the USDA National Institute of Food and Agriculture, Agricultural and Food Research Initiative Competitive Programme, Ecosystem Services and Agro-ecosystem Management, Grant No. 2018-67019-27850. A.T.T. acknowledges support from the USDA National Institute of Food and Agriculture Postdoctoral Research Fellowship Grant No. 2018-67012-28020.

References

AbdElgawad H, Farfan-Vignolo ER, de Vos D, Asard H (2015) Elevated CO_2 mitigates drought and temperature-induced oxidative stress differently in grasses and legumes. Plant Sci 231:1–10.

Adams HD, Guardiola-Claramonte M, Barron-Gafford GA, Villegas JC, Breshears DD, Zou CB, Troch PA, Huxman TE (2009) Temperature sensitivity of drought-induced tree mortality portends increased regional die-off under global-change-type drought. Proc Natl Acad Sci USA 106:7063–7066.

Adams HD, Zeppel MJB, Anderegg WRL et al. (2017) A multi-species synthesis of physiological mechanisms in drought-induced tree mortality. Nat Ecol Evol 1:1285–1291.

Ainsworth EA, Long SP (2005) What have we learned from 15 years of free-air CO_2 enrichment (FACE)? A meta-analytic review of the responses of photosynthesis, canopy properties and plant production to rising CO_2. New Phytol 165:351–372.

Alder NN, Pockman WT, Sperry JS, Nuismer S (1997) Use of centrifugal force in the study of xylem cavitation. J Exp Bot 48:665–674.

Allen CD, Macalady AK, Chenchouni H et al. (2010) A global overview of drought and heat-induced tree mortality reveals emerging climate change risks for forests. For Ecol Manage 259:660–684.

Anderegg WRL, Schwalm C, Biondi F et al. (2015) Pervasive drought legacies in forest ecosystems and their implications for carbon cycle models. Science 349:528–532.

Anderegg WRL, Klein T, Bartlett M, Sack L, Pellegrini AFA, Choat B (2016) Meta-analysis reveals that hydraulic traits explain cross-species patterns of drought-induced tree mortality across the globe. Proc Natl Acad Sci USA 113:2–7.

Anderegg WRL, Wolf A, Arango-Velez A et al. (2017) Plant water potential improves prediction of empirical stomatal models. PLoS One 12:e0185481.

Anderegg WRL, Wolf A, Arango-Velez A et al. (2018) Woody plants optimise stomatal behaviour relative to hydraulic risk. Ecol Lett 21:968–977.

Ball JT, Woodrow IE, Berry JA (1987) A model predicting stomatal conductance and its contribution to control of phosynthesis under different environmental conditions. In: Biggins J. (eds) Progress in photosynthesis research. Springer, Dordrecht, pp 221–224.

Bartlett MK, Zhang Y, Kreidler N, Sun S, Ardy R, Cao K, Sack L (2014) Global analysis of plasticity in turgor loss point, a key drought tolerance trait. Ecol Lett 17:1580–1590.

Buckley TN (2017) Modeling stomatal conductance. Plant Physiol 174:572–582.

Buckley TN, Schymanski SJ (2014) Stomatal optimisation in relation to atmospheric CO_2. New Phytol 201:372–377.

Buckley TN, Sack L, Farquhar GD (2017) Optimal plant water economy. Plant Cell Environ 40:881–896.

Chen Z, Hills A, Batz U, Amtmann A, Lew VL, Blatt MR (2012) Systems dynamic modelling of the stomatal guard cell predicts emergent behaviours in transport, signalling and volume control. Plant Physiol 159:1235–1251.

Cowan IR, Farquhar GD (1977) Stomatal function in relation to leaf metabolism and environment. Symp Soc Exp Biol 31:471–505.

De Kauwe MG, Medlyn BE, Zaehle S et al. (2013) Forest water use and water use efficiency at elevated CO_2: a model-data intercomparison at two contrasting temperate forest FACE sites. Glob Chang Biol 19:1759–1779.

Dewar R, Mauranen A, Mäkelä A, Hölttä T, Medlyn B, Vesala T (2018) New insights into the covariation of stomatal, mesophyll and hydraulic conductances from optimization models incorporating nonstomatal limitations to photosynthesis. New Phytol 217:571–585.

Drake JE, Power SA, Duursma RA et al. (2017) Stomatal and non-stomatal limitations of photosynthesis for four tree species under

drought: a comparison of model formulations. Agric For Meteorol 247:454–466.
Eissenstat DM, Wells CE, Yanai RD, Whitbeck JL (2000) Building roots in a changing environment: implications for root longevity. New Phytol 147:33–42.
Flexas J, Ribas-Carbó M, Diaz-Espejo A, Galmés J, Medrano H (2008) Mesophyll conductance to CO_2: current knowledge and future prospects. Plant Cell Environ 31:602–621.
Gonzalez-Benecke CA, Teskey RO, Dinon-Aldridge H, Martin TA (2017) *Pinus taeda* forest growth predictions in the 21st century vary with site mean annual temperature and site quality. Glob Chang Biol 23:4689–4705.
Guswa AJ (2008) The influence of climate on root depth: a carbon cost-benefit analysis. Water Resour Res 44:W02427.
Hacke UG, Sperry JS, Pittermann J (2000) Drought experience and cavitation resistance in six shrubs from the Great Basin, Utah. Basic Appl Ecol 1:31–41.
Hacke UG, Venturas MD, Mackinnon ED, Jacobsen AL, Sperry JS, Pratt RB (2015) The standard centrifuge method accurately measures vulnerability curves of long-vesselled olive stems. New Phytol 205: 116–127.
Hills A, Chen Z, Amtmann A, Blatt MR, Lew VL (2012) OnGuard, a computational platform for quantitative kinetic modelling of guard cell physiology. Plant Physiol 159:1026–1042.
Huang C-W, Domec J-C, Palmroth S, Pockman WT, Litvak ME, Katul GG (2018) Transport in a coordinated soil-root-xylem-phloem leaf system. Adv Water Resour 119:1–16.
Hubbard RM, Ryan MG, Stiller V, Sperry JS (2001) Stomatal conductance and photosynthesis vary linearly with plant hydraulic conductance in ponderosa pine. Plant Cell Environ 24:113–121.
IPCC (2014) Climate change 2014: synthesis report. Core Writing Team, RK Pachauri and LA Meyer (eds) Contribution of Working Groups I, II and III to the Fifth Assessment Report of the Intergovernmental Panel on Climate Change. IPCC, Geneva, Switzerland.
Katul G, Manzoni S, Palmroth S, Oren R (2010) A stomatal optimization theory to describe the effects of atmospheric CO_2 on leaf photosynthesis and transpiration. Ann Bot 105:431–442.
Katul GG, Palmroth S, Oren R (2009) Leaf stomatal responses to vapour pressure deficit under current and CO_2-enriched atmosphere explained by the economics of gas exchange. Plant Cell Environ 32:968–979.
Kolb KJ, Sperry JS, Lamont BB (1996) A method for measuring xylem hydraulic conductance and embolism in entire root and shoot systems. J Exp Bot 47:1805–1810.
Leuning R (1995) A critical appraisal of a combined stomatal-photosynthesis model for C_3 plants. Plant Cell Environ 18: 339–355.
Mackay DS, Roberts DE, Ewers BE, Sperry JS, McDowell NG, Pockman WT (2015) Interdependence of chronic hydraulic dysfunction and canopy processes can improve integrated models of tree response to drought. Water Resour Res 51:6156–6176.
Manzoni S, Vico G, Palmroth S, Porporato A, Katul G (2013) Optimization of stomatal conductance for maximum carbon gain under dynamic soil moisture. Adv Water Resour 62:90–105.
McDowell NG, Fisher RA, Xu C et al. (2013) Evaluating theories of drought-induced vegetation mortality using a multimodel-experiment framework. New Phytol 200:304–321.
Medlyn BE, Duursma RA, Eamus D, et al. (2011) Reconciling the optimal and empirical approaches to modelling stomatal conductance. Glob Chang Biol 17:2134–2144.
Meinzer FC, Woodruff DR, Marias DE, Smith DD, McCulloh KA, Howard AR, Magedman AL (2016) Mapping 'hydroscapes' along the iso- to anisohydric continuum of stomatal regulation of plant water status. Ecol Lett 19:1343–1352.
Nikinmaa E, Hölttä T, Hari P, Kolari P, Mäkelä A, Sevanto S, Vesala T (2013) Assimilate transport in phloem sets conditions for leaf gas exchange. Plant Cell Environ 36:655–669.
Pataki DE, Oren R, Phillips N (1998) Responses of sap flux and stomatal conductance of *Pinus taeda* L. trees to stepwise reductions in leaf area. J Exp Bot 49:871–878.
Powell TL, Galbraith DR, Christoffersen BO et al. (2013) Confronting model predictions of carbon fluxes with measurements of Amazon forests subjected to experimental drought. New Phytol 200:350–365.
Santiago LS, Goldstein G, Meinzer FC, Fisher JB, Machado K, Woodruff D, Jones T (2004) Leaf photosynthetic traits scale with hydraulic conductivity and wood density in Panamanian forest canopy trees. Oecologia 140:543–550.
Scoffoni C, Albuquerque C, Brodersen CR, Townes SV, John GP, Bartlett MK, Buckley TN, McElrone AJ, Sack L (2017) Outside-xylem vulnerability, not xylem embolism, controls leaf hydraulic decline during dehydration. Plant Physiol 173:1197–1210.
Sperry JS (2000) Hydraulic constraints on plant gas exchange. Agric For Meteorol 104:13–23.
Sperry JS, Love DM (2015) What plant hydraulics can tell us about responses to climate-change droughts. New Phytol 207:14–27.
Sperry JS, Saliendra NZ (1994) Intra- and inter-plant variation in xylem cavitation in *Betula occidentalis*. Plant Cell Environ 17: 1233–1241.
Sperry JS, Donnelly JR, Tyree MT (1988) A method for measuring hydraulic conductivity and embolism in xylem. Plant Cell Environ 11:35–40.
Sperry JS, Adler FR, Campbell GS, Comstock JP (1998) Limitation of plant water use by rhizosphere and xylem conductance: results from a model. Plant Cell Environ 21:347–359.
Sperry JS, Wang Y, Wolfe BT, Mackay DS, Anderegg WRL, McDowell NG, Pockman WT (2016) Pragmatic hydraulic theory predicts stomatal responses to climatic water deficits. New Phytol 212:577–589.
Sperry JS, Venturas MD, Anderegg WRL, Mencuccini M, Mackay DS, Wang Y, Love DM (2017) Predicting stomatal responses to the environment from the optimization of photosynthetic gain and hydraulic cost. Plant Cell Environ 40:816–830.
Tai X, Mackay DS, Anderegg WRL, Sperry JS, Brooks PD (2017) Plant hydraulics improves and topography mediates prediction of aspen mortality in southwestern USA. New Phytol 213:113–127.
Torres-Ruiz JM, Sperry JS, Fernández JE (2012) Improving xylem hydraulic conductivity measurements by correcting the error caused by passive water uptake. Physiol Plant 146:129–135.
Trugman AT, Detto M, Bartlett MK, Medvigy D, Anderegg WRL, Schwalm C, Schaffer B, Pacala SW (2018*a*) Tree carbon allocation explains forest drought-kill and recovery patterns. Ecol Lett 21: 1552–1560.
Trugman AT, Medvigy D, Mankin JS, Anderegg WRL (2018*b*) Soil moisture stress as a major driver of carbon cycle uncertainty. Geophys Res Lett 45:6495–6503.
Tuzet A, Perrier A, Leuning R (2003) A coupled model of stomatal conductance, photosynthesis and transpiration. Plant Cell Environ 26:1097–1116.
Venturas MD, Sperry JS, Love DM, Frehner EH, Allred MG, Wang Y, Anderegg WRL (2018) A stomatal control model based on optimization of carbon gain versus hydraulic risk predicts aspen sapling responses to drought. New Phytol 220:836–850.
Walker A, Hanson P, De Kauwe MG et al. (2014) Comprehensive ecosystem model-data synthesis using multiple data sets at two temperate forest free-air CO_2 enrichment experiments: model performance at ambient CO_2 concentration. J Geophys Res Biogeo sci 119:937–964.

Wolf A, Anderegg WRL, Pacala SW (2016) Optimal stomatal behavior with competition for water and risk of hydraulic impairment. Proc Natl Acad Sci USA 113:E7222–E7230.

Wolfe BT, Sperry JS, Kursar TA (2016) Does leaf shedding protect stems from cavitation during seasonal droughts? A test of the hydraulic fuse hypothesis. New Phytol 212:1007–1018.

Zinta G, Abdelgawad H, Domagalska MA, Vergauwen L, Knapen D, Nijs I, Janssens IA, Beemster GTS, Asard H (2014) Physiological, biochemical, and genome-wide transcriptional analysis reveals that elevated CO_2 mitigates the impact of combined heat wave and drought stress in *Arabidopsis thaliana* at multiple organizational levels. Glob Chang Biol 20:3670–3685.